

# Characterizing the effect of elastic interactions on the effective elastic properties of porous, cracked rocks

Luanxiao Zhao<sup>1,2\*</sup>, Qiuliang Yao<sup>2</sup>, De-hua Han<sup>2</sup>, Fuyong Yan<sup>2</sup>  
and Mosab Nasser<sup>3,2</sup>

<sup>1</sup>State Key Laboratory of Marine Geology, Tongji University, Shanghai, China, <sup>2</sup>Department of Earth and Atmospheric Sciences, University of Houston, Houston, USA, and <sup>3</sup>Maersk Oil America Inc., Houston, USA

Received November 2013, revision accepted December 2014

## ABSTRACT

Elastic interactions between pores and cracks reflect how they are organized or spatially distributed in porous rocks. The principle goal of this paper is to understand and characterize the effect of elastic interactions on the effective elastic properties. We perform finite element modelling to quantitatively study how the spatial arrangement of inclusions affects stress distribution and the resulting overall elasticity. It is found that the stress field can be significantly altered by elastic interactions. Compared with a non-interacting situation, stress shielding considerably stiffens the effective media, while stress amplification appreciably reduces the effective elasticity. We also demonstrate that the T-matrix approach, which takes into account the ellipsoid distribution of pores or cracks, can successfully characterize the competing effects between stress shielding and stress amplification. Numerical results suggest that, when the concentrations of cracks increase beyond the dilute limit, the single parameter crack density is not sufficient to characterize the contribution of the cracks to the effective elasticity. In order to obtain more reliable and accurate predictions for the effective elastic responses and seismic anisotropies, the spatial distribution of pores and cracks should be included. Additionally, such elastic interaction effects are also dependent on both the pore shapes and the fluid infill.

**Key words:** Elastic interaction, Porous, Modelling.

## INTRODUCTION

Sedimentary rocks are generally porous and often fractured or cracked to some extent. Understanding their elastic behaviour is essential to interpret and predict sonic measurements and seismic responses in terms of rock properties. This understanding comes primarily from effective medium theories that relate the microstructural parameters of rocks (mineral composition, porosity, microstructure, etc.) to the effective elastic responses (Guéguen and Kachanov 2011). Consequently, many theoretical models have emerged, seeking to predict the effective elastic properties in porous, cracked media. Most of

them are based on strong assumptions with idealizations and simplification of the complexity of real rocks.

The most popular approaches use non-interaction approximation (NIA) to predict the overall compressibility of rocks containing finite concentrations of pores and cracks, owing to the difficulty of solving elastic interactions between pores and cracks. Pioneering work concerning NIA was initiated by the paper of Eshelby (1957), in which he presented the solution to the strain field of an ellipsoidal inclusion in an infinite, homogeneous solid. Generally, there are two approaches to formulate the NIA theory. The first type of NIA approach directly estimates the effective stiffness as a function of porosity and crack density (Walsh 1965; O'Connell and Budiansky 1974; Kuster and Toksöz 1974; Hudson 1980, 1981, 1994).

---

\*Email: zhaoluanxiao@gmail.com

Walsh (1965) predicted the compressibility of dry rocks with spherical pores and narrow cracks and found that pore shapes and their volume concentration can be combined to affect the overall elasticity. By applying a long wavelength, first-order scattering theory, Kuster and Toksöz (1974) calculated the effective moduli for randomly oriented inclusions. Their results are considered to be valid only for a small-volume fraction of inclusions, since the multiple scattering effects are ignored in their methods. Based on a scattering-theory analysis of the mean wavefield in an elastic solid with thin, penny-shaped ellipsoidal cracks or inclusions, Hudson derived the first-order correction and second-order correction to compute the effective moduli of the cracked media (Hudson 1980, 1981, 1994). The first-order Hudson's model that ignores the crack interactions can only work at low crack density. The second-order expansion of Hudson's model takes into account the pair-wise interactions between cracks but gives an unphysical prediction at high crack density. The dilute limit in Hudson's theory for both the first- and second-order terms is less than 0.1.

The second type of NIA approach considers the effective compliance as a sum of the contributions from the matrix compliance and excess compliances from pores and cracks (Schoenberg 1980, 1983; Kachanov 1992; Kachanov, Tsukrov and Shafiro 1994; Sayers and Kachanov 1995; Liu, Hudson and Pointer 2000; Kachanov, Shafiro and Tsukrov 2003; Grechka and Kachanov 2006; Vernik and Kachanov 2010). Kachanov (1992) and Kachanov *et al.* (2003) concluded that compliance-based NIA remains sufficiently accurate at large crack density and strong interactions. They stated that the two competing interaction effects of stress shielding and stress amplification can counteract and cancel each other, so the pore and crack interactions can be neglected. Another argument for the proponents of the compliance-based NIA is that this theory can yield reasonable estimates at high volume concentration of pores and cracks, while the stiffness-based NIA typically fails. Rather than assuming that the fracture is a cluster of penny-shaped cracks, Schoenberg (1980, 1983) suggested to describe the fractures as planes of weakness with linear-slip boundary conditions and the relations between the geometry of penny-shaped cracks and the fracture compliance were derived by Schoenberg and Douma (1988) and Sayers and Kachanov (1995).

So far, we have to bear in mind that the above mentioned NIA inclusion and crack theories ignore the elastic interactions between pores and cracks. Hence, theoretically, they can work only for dilute concentrations. However, these dilute limits (roughly, porosity less than 10 per cent, crack density less than 0.1) make the NIA theory not applicable for many sedimentary rocks. To overcome the dilute limit of

NIA, it is of great interest to study how the pore and crack interactions affect the elastic behaviours of rocks.

To put it more specifically, pore and crack interactions reflect how pores and cracks are organized or spatially distributed. As we know, the geometrical arrangement of pores and cracks can have large variations due to their deposition and diagenesis during the geological history. Physically, such spatial distributions and correlations of pores and cracks can affect the local stress field and the resulting overall elastic properties. In order to study the effect of pore and crack interactions, some rock physics schemes, such as the self-consistent (SC) theory (Budiansky 1965; Hill 1965; Wu 1966; Berryman 1980a, 1980b, 1995; Hornby, Schwartz and Hudson 1994) and differential effective medium (DEM) theory (Nishizawa 1982; Norris 1985; Zimmerman 1991; Berryman 1992; Hornby *et al.* 1994; Xu 1998), are proposed to handle large concentrations of pores and cracks. These two rock physics schemes, simulating the pore and crack interactions in an implicit way, are relatively successful and have certainly been popular in the past decades. An important conceptual difference between the DEM and SCA schemes is that the DEM scheme treats each constituent asymmetrically with a preferred host matrix, whereas the SCA scheme does not identify any specific host material but treats the composite as an aggregate of all the constituents (Mavko, Mukerji and Dvorkin 2009). In contrast to DEM and SC that consider the elastic interactions implicitly, Jakobsen (2004), Jakobsen and Chapman (2009) and Jakobsen, Hudson and Johansen (2003) formulated the effective stiffness using T-matrix language to explicitly characterize the pore and crack interactions.

The paper is organized as follows: first, we perform finite element modelling to study how elastic interactions (stress amplification and stress shielding) affect stress field distribution and the resulting overall elasticity. We then introduce the T-matrix theory, which explicitly simulates elastic interactions and investigate the influence of the spatial distribution of pores and cracks on the effective stiffness. We next numerically compare the performance of different effective medium theories in modelling elastic responses and the resulting anisotropies of porous, cracked rock. We end with discussions and conclusions.

## NUMERICAL EXPERIMENT ON STRESS INTERACTION

In this section, finite-element modelling (Software COMSOL) is employed to investigate stress interactions between cracks. We simulate remote stress boundary conditions by applying a constant load (70 000 Pa) to a homogeneous 2D solid matrix

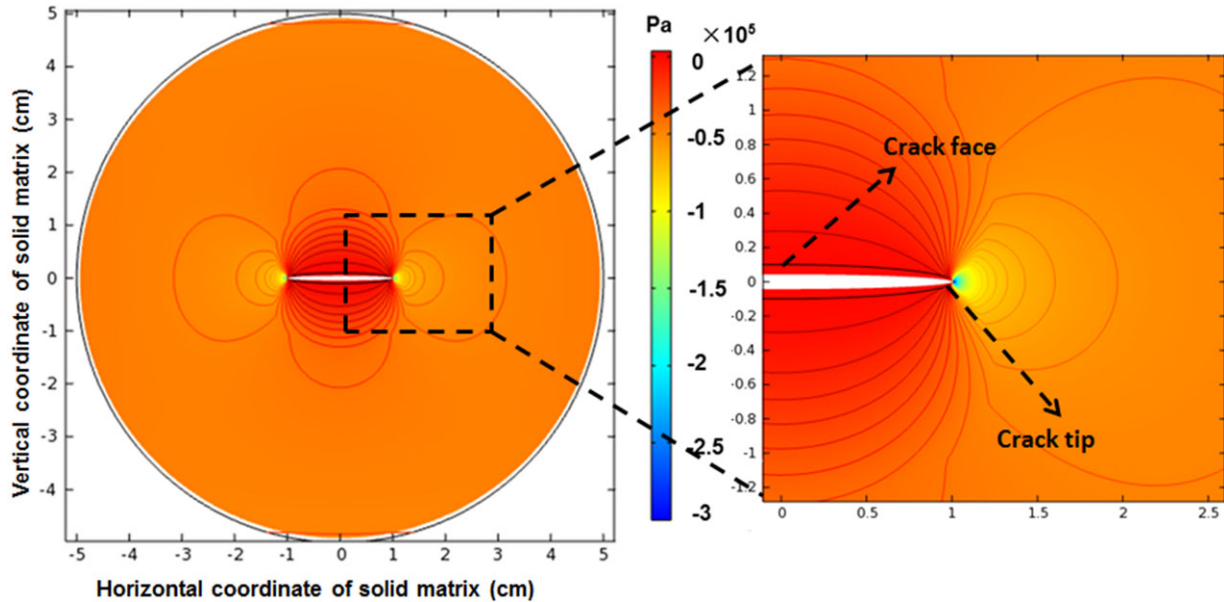


**Figure 1** First principal stress distribution of one crack in a homogeneous solid matrix. To the right, the stress field around the tips of the crack are zoomed-in. The iso-stress lines that are present around the crack represent the variation of the stress field magnitude. Note the stress concentration occurs at the crack tip and stress dilution occurs at the crack face. The host solid matrix has 2D circle geometry (radius = 5 cm). The colour-bar indicates the magnitude of stress in Pa.

( $E = 70$  GPa,  $\nu = 0.33$ ) with a radius of 5 cm. The aspect ratio of the ellipsoidal inclusion is set to 0.1 to mimic the geometry of the crack. Instead of a uniform stress field, the existence of the crack alters the stress distribution in its vicinity, as shown in Fig. 1. It turns out that the alteration of the stress field is strongly localized. The high density of iso-stress lines near crack tips suggests that the stress magnitude varies strongly around crack tips. Also, the colour bar clearly indicates a stress concentration (stress magnitude is greater than the background) near the crack tips and a stress dilution (stress magnitude is less than the background) near the crack faces. In Fig. 2, we plot the detailed stress magnitude values along two straight lines crossing the centre of the crack vertically and horizontally. First, the stress field inside the elliptical crack is considered to be uniform and approximates to zero when the crack is dry or filled with gas. Second, at the locations far away from the crack, the values of the stress magnitude on both lines are close to each other, because they are almost not affected by the introduction of the crack. Finally, when approaching towards the tips and faces of the crack, it is interesting to see that the resulting stress fields exhibit distinct behaviours. Along the defined horizontal coordinate, the stress magnitude increases dramatically to about  $-3 \times 10^5$  Pa when close to the crack tip, then abruptly drops to zero. By contrast, along the defined vertical coordinate, the stress

**Table 1** Comparison of a normalized volumetric strain that corresponds to different stress interaction situations in Fig. 3.

No cracks	Non-interaction	Stress Shielding	Stress Amplification
1	13.2	9.3	17.1

magnitude gradually reduces to 0 Pa when close to the crack face, evidently suggesting that a stress dilution dominates the stress field.

In the next numerical experiment, we introduce two cracks into the matrix, with three different spatial arrangements, to illustrate three types of stress interactions, which are non-interaction, stress amplification and stress shielding respectively (Fig. 3). Applying the same constant load in all three cases, we also calculate the total volumetric strains, normalized to the volumetric strain of the matrix (without cracks) and compare them in Table 1. Figure 3(a) shows the stress distribution when the two introduced cracks are far apart from each other, to mimic the non-interacting situation. It seems that the stress field of the one crack does not affect the stress field of the other crack, so the overall elastic interactions between the two cracks are trivial. As shown in Table 1, the normalized volumetric strain consequently increases from 1

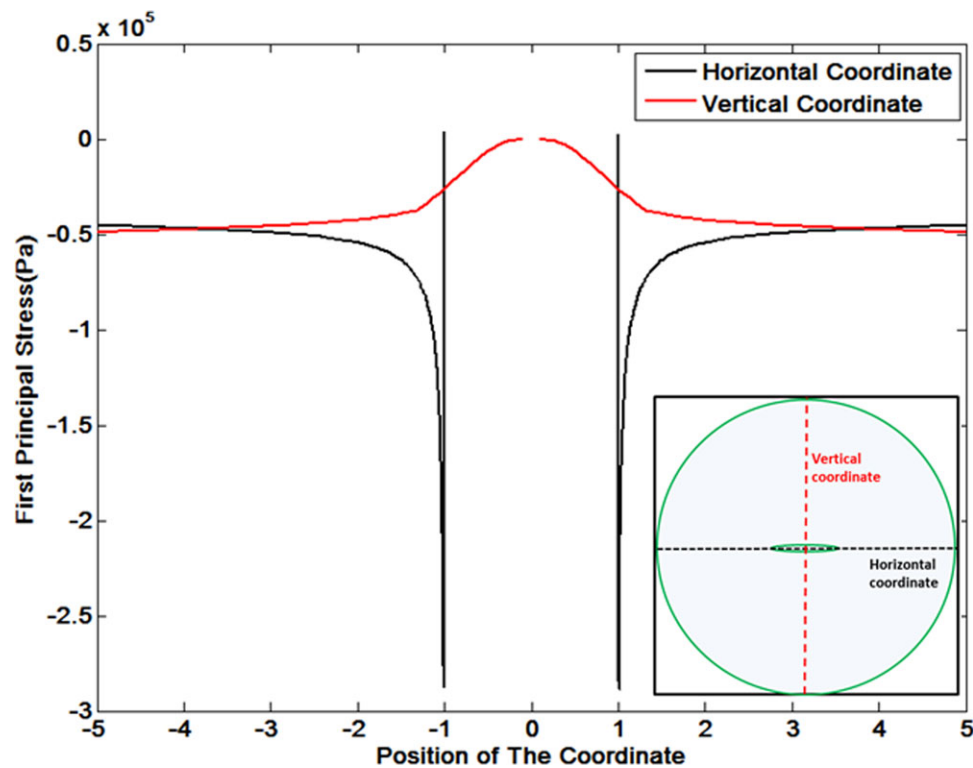


**Figure 2** The variation of the first principal stress of a single crack with the positions of the horizontal coordinate (black line) and vertical coordinate (red line). The horizontal coordinate is defined as the line between the two points  $(-5, 0)$  and  $(5, 0)$ ; the vertical coordinate is defined as the line between the two points  $(0, -5)$  and  $(0, 5)$ . A schematic illustration of the horizontal and vertical coordinates is displayed in the bottom-right corner.

to 13.2 due to the extra strain of the two non-interacting cracks. Figure 3(b) shows the stress distribution due to a set of coplanar cracks when crack tips approach closely to each other. As expected, the stress is concentrated at the area between the tips of the cracks. The stress amplification is clearly illustrated in Fig. 4(a). Along the horizontal coordinate, the stresses magnitudes between the two neighbouring tips increase to much higher values compared to those beside the two isolated tips. Along the vertical coordinate, the stress interaction transits from stress shielding to stress amplification when approaching the centre point between the two cracks. It is also interesting to note that the maximum local stress magnitude does not occur at the exact midway between the two cracks. Actually, there exist two maximums that symmetrically occur very close to the tips. In this case, the resulting volumetric strain increases to 17, which is higher than the non-interacting situation. This is because the stress amplification dominates the stress interaction and thus increases the overall strain. Figures 3(c) and 4(b) show the stress field distribution due to the set of stacked cracks, where the stress shielding dominates the stress interaction when the crack faces

approach closely to each other. It is clear that the overall stress magnitude is much lower than that due to the set of coplanar cracks and the local stress magnitude at the tip of each crack is much stronger than that occurring at the centre of the tips between the two cracks. As illustrated in Fig. 4(b), as the position moves from the far-field to the area between the two stacked cracks along the horizontal coordinate, the stress interaction becomes complicated and varies strongly with the location. However, it is interesting to note that the values of stress magnitude in the majority of the area between the two cracks are very close to zero. This is a clear indication that the stresses fields are shielded between the two cracks when their faces are close to each other. Since the tips are also closer to each other in this case, there certainly exists a competing effect between the stress amplification and the stress shielding but the overall stress interaction is still controlled by stress shielding. As shown in Table 1, the volumetric strain due to the set of stacked cracks decreases considerably compared with the non-interacting case. Consequently, it can be concluded that the effective stiffness tends to be higher when stress shielding dominates the stress interactions, while the effective stiffness

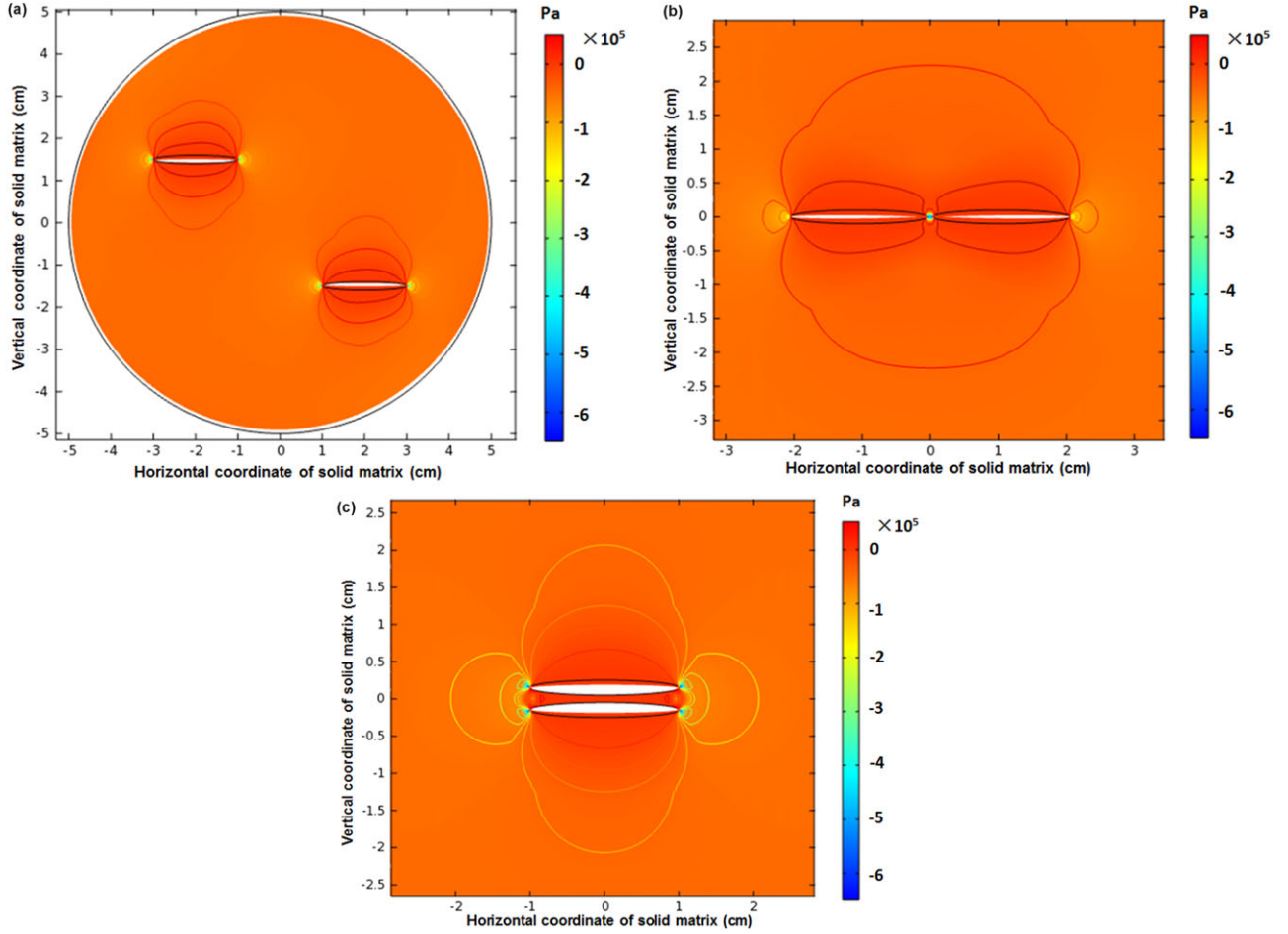


**Figure 3** Comparison of the first principal stress distribution by introducing different sets of cracks into the homogeneous solid matrix: (a) cracks are far apart from each other, which is considered as a non-interaction situation, (b) coplanar cracks where stress amplification dominates the stress interaction and (c) stacked cracks where stress shielding dominates the stress interaction. The iso-stress lines represent the variation of the stress field magnitude for the different cases of stress interactions. The colour-bar indicates the magnitude of stress in Pa.

tends to be lower when stress amplification dominates the stress interactions.

## T-MATRIX TO CHARACTERIZE ELASTIC INTERACTIONS

As illustrated in the previous section, the impacts of stress shielding and stress amplification on the overall effective stiffness depend on the spatial arrangements of the pores and cracks. Therefore it is necessary to find a way to explicitly characterize such spatial arrangements in order to properly model the elastic interactions. In this section, we investigate how the T-matrix approach captures the elastic characteristic due to different spatial distributions of pores and cracks.

## T-matrix formulation

Based on multiple-point correlation functions, the T-matrix language explicitly takes into account the elastic interactions between inclusions to compute the effective elastic properties. The effective stiffness  $C_T^*$  of a cracked, porous medium using the T-matrix approach was formulated by Jakobsen (2004) and Jakobsen *et al.* (2003):

$$C_T^* = C^0 + \langle T_1 \rangle (I - \langle T_1 \rangle^{-1} X)^{-1}, \quad (1)$$

where

$$\langle T_1 \rangle = \sum_{r=1}^N v^r t^r, \quad (2)$$

$$t^r = \delta C^r (I - G^r \delta C^r)^{-1}, \quad (3)$$

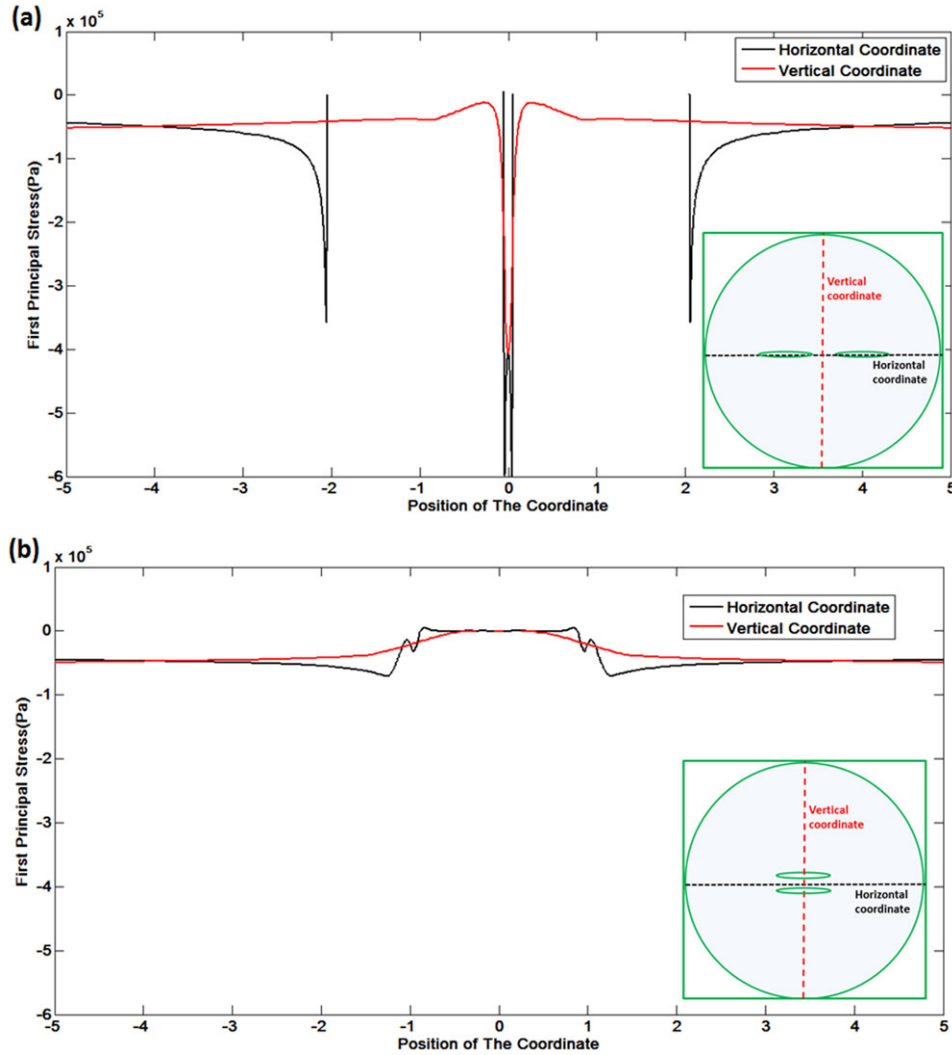


**Figure 4** The variation of the first principal stress with the positions of the horizontal coordinate (black line) and vertical coordinate (red line) for the case of: (a) coplanar cracks, (b) stacked cracks. The horizontal coordinate is defined as the line between the two points  $(-5, 0)$  and  $(5, 0)$ ; the vertical coordinate is defined as the line between the two points  $(0, -5)$  and  $(0, 5)$ . A schematic illustration of the horizontal and vertical coordinates is displayed in the bottom-right corners.

and

$$\delta C^r = C^r - C^0. \quad (4)$$

Here,  $C^0$  is the fourth-rank stiffness of the host rock;  $v^r$  is the volume fraction of the inclusions ( $r = 1, 2, \dots, N$ );  $C^r$  represents the stiffness tensor of the  $r$ th inclusion;  $I$  is the fourth-rank identity tensor;  $G^r$  is a fourth-rank tensor given by the strain Green's function integrated over the characteristic inclusion shape (Mura 1987);  $X$  is the second-order correction for the effects of an inclusion tensor:

$$X = - \sum_{r=1}^N \sum_{s=1}^N v^r t^r G_d^{rs} v^s t^s, \quad (5)$$

where  $G_d^{rs}$  represents the two-point interaction between the  $r$ th set and  $s$ th set of inclusions. The fourth-rank tensor  $G_d^{rs}$  can be obtained in the same way as  $G^r$  except that the aspect ratio of the inclusion  $\alpha_r$  is set as the aspect ratio of spatial distribution  $\alpha_d$ .

The definitions of the aspect ratio of inclusion  $\alpha_r$  and the aspect ratio of spatial distribution  $\alpha_d$  are schematically displayed in Fig. 5. In fact, the concept of the aspect ratio of spatial distribution represents the conditional probability of finding another inclusion given the position of an inclusion. Figure 6 shows that an individual crack in two rocks has the same aspect ratio but organized in a different way. If  $\alpha_d < 1$ ,

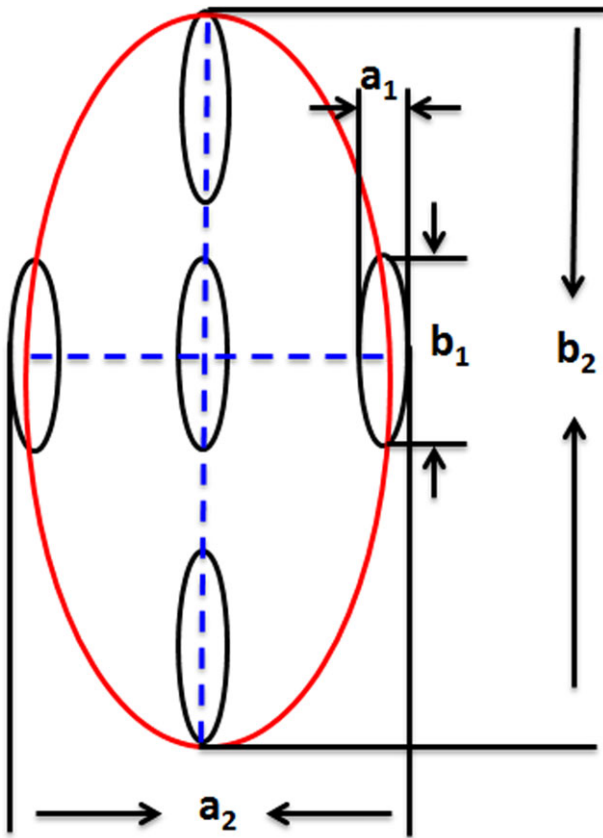


Figure 5 Schematic illustration of a 2D cross-section through a 3D ellipsoidal crack distribution in a T-matrix model. The aspect ratio of the individual cracks is  $a_1/b_1$  and the aspect ratio of the crack distribution is  $a_2/b_2$ .

it indicates that the probability of an inclusion showing up in the X direction is higher than the probability of finding an inclusion in the Y direction. Ponte-Castaneda and Willis (1995) pointed out that the maximum value for an aspect ratio of spatial distribution  $\alpha_d$  should satisfy the relationship  $\alpha_{d(\max)} = \alpha_r/v$ , where  $v$  is the volume concentration of inclusions.

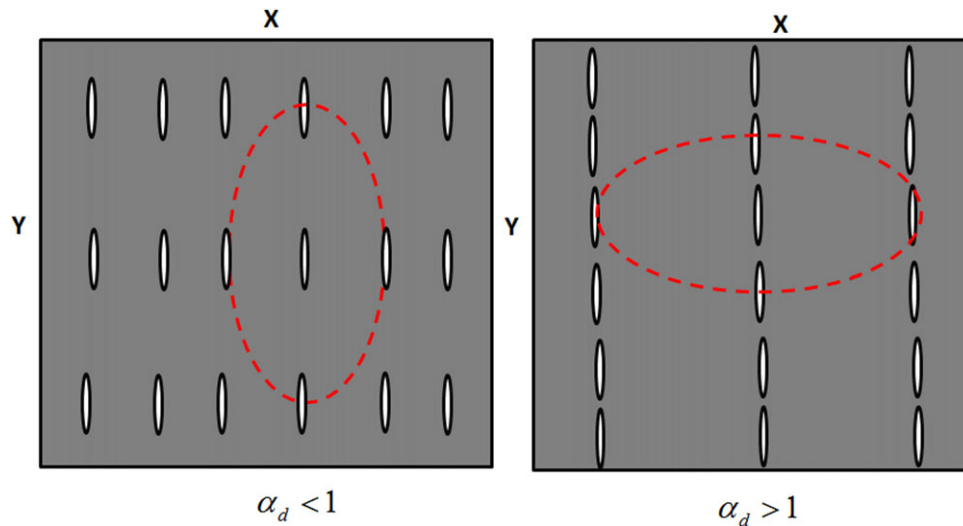
Comparisons of the effective stiffness C11, C33, C44, C66 and C13 as a function of crack density predicted by the T-matrix are displayed in Fig. 7. In our modelling, cracks are vertically aligned and parallel to each other in an isotropic host rock and the resultant cracked rock is transversely isotropic with a horizontal symmetry axis (HTI). The host matrix is assumed to be calcite ( $K = 76.8\text{GPa}$ ,  $\mu = 32\text{GPa}$ ). There are five independent components in the effective elastic stiffness tensors: C11 and C33 correspond to the P-wave propagating perpendicular and parallel to the crack plane, respectively; C44 and C66 are related to the polarization of the

S-wave parallel and perpendicular to the crack plane, respectively; C13 is intimately associated with the P-wave velocity at  $45^\circ$  to the symmetry axis. The volume crack density  $\varepsilon$  (O'Connell and Budiansky 1974; Hudson 1980) is determined by the crack aspect ratio and the crack induced porosity. In Fig. 7, the dashed straight lines represent the first-order T-matrix (stiffness-based NIA) predictions and the solid lines, exhibiting a non-linear relationship with crack density, are for the high-order T-matrix predictions taking into account the elastic interactions. C11 and C33, predicted by stiffness-based NIA, typically break down when the crack density is over 0.15. However, the high-order T-matrix can still provide reasonable estimates even at high crack density. They overlap at a crack density less than 0.02 but are markedly separated at high crack density, where the elastic interactions are considered to be strong and cannot be ignored.

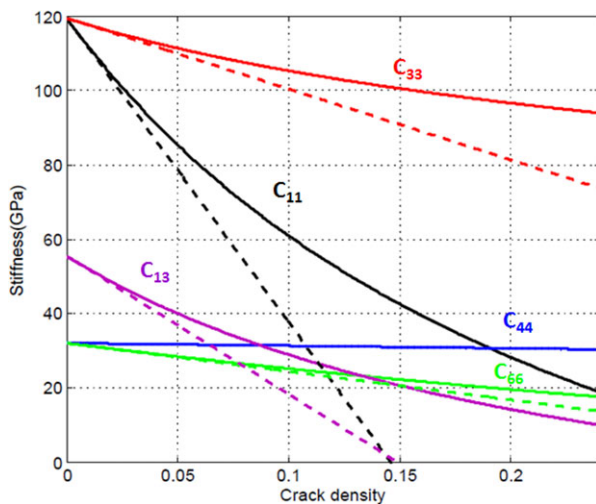
#### Effect of spatial distribution on effective stiffness

Figure 8 illustrates the influences of the aspect ratio of the inclusion and the aspect ratio of spatial distribution on the stiffness of C11. Clearly, compared with the aspect ratio of spatial distribution, the aspect ratio of inclusion still has a dominant impact on controlling the rock's overall elastic behaviour. It is also interesting to see that the elastic stiffness exhibits a different sensitivity to the aspect ratio of spatial distribution when the aspect ratio of inclusion varies. Generally, the aspect ratio of spatial distribution has a bigger impact on the effective elastic stiffness when the aspect ratio of inclusion is lower. This is because when the aspect ratio of the crack is smaller, the local stress field can readily exhibit concentration and dilution and the stress interactions consequently exercise a bigger influence on the elastic properties. We can also conclude that the computed elastic stiffness decreases with an increasing aspect ratio of spatial distribution. This can be explained by the variation of stress field due to the crack interactions. When the aspect ratio of the spatial distribution increases, the crack tips will approach closer and closer. As a result, the stress amplification will increase much stronger than the stress shielding and the effective elastic stiffness will decrease accordingly. This is consistent with the numerical experiment about the stress interactions we presented in Fig. 3. Furthermore, it demonstrates that the parameter 'aspect ratio of spatial distribution' can successfully characterize the competing effects between stress shielding and amplification.

We also evaluated the interaction effects on both dry and brine filled cracks and compare them in Fig. 8(a,b). The



**Figure 6** Schematic illustration of the concept of the aspect ratio of spatial distribution. Each individual crack has the same aspect ratio but organized in a different way. The red circle indicates the aspect ratio of spatial distribution: (left) the aspect ratio of spatial distribution is smaller than 1; (right) the aspect ratio of spatial distribution is bigger than 1.



**Figure 7** Effective elastic properties of cracked carbonate as a function of crack density.  $C_{11}$ ,  $C_{33}$ ,  $C_{13}$ ,  $C_{44}$  and  $C_{66}$  represent five independent elastic stiffness constants in HTI medium. The dashed and solid lines indicate the effective elastic stiffness predicted by a first-order T-matrix and a high-order T-matrix, respectively. The aspect ratio of the crack is set as 0.05 and the aspect ratio of spatial distribution is set as 1.0.

results show that, for the brine filled cracks, the elastic stiffness  $C_{11}$  has less sensitivity to the variation of the aspect ratio of spatial distribution. Physically, this makes sense because the brine often drastically stiffens the very compliant cracks (Schoenberg and Sayers 1995). As a consequence, the stress interactions are becoming weaker and have less impact on the effective elastic stiffness.

## COMPARISON OF DIFFERENT EFFECTIVE MEDIUM THEORIES

To gain insights into the advantages and limitations of various effective medium theories, we compare the performances of the T-matrix with Hudson's crack theory, compliance-based non-interaction approximation, SCA and differential effective medium model, as displayed in Fig. 9. As expected, several predictions largely agree with each other when the crack density is low but there are significant differences at high crack density. Again, this illustrates the importance of including the effects of spatial distribution when coping with non-dilute concentrations of pores and cracks. Evidently, at high crack density, the prediction given by Hudson's crack theory (stiffness-based NIA) typically breaks down and it becomes close to the T-matrix's estimates when stress amplification makes a dominant impact. The compliance-based NIA gives the best match with the T-matrix when the aspect ratio of spatial distribution is very small, which represents the crack interaction effect dominated by stress shielding. However, this should not be treated as physical equivalence. The compliance-based NIA does not take into consideration the crack interactions. Nonetheless, those pore and crack interactions are explicitly characterized in the T-matrix formulation. An additional insight that can be gained from this comparison is that the SCA and DEM prediction approaches the T-matrix prediction when the aspect ratio of the spatial distribution is 1. This is in agreement with the assumption of SCA and DEM, in which the cracks are randomly distributed and interacted.

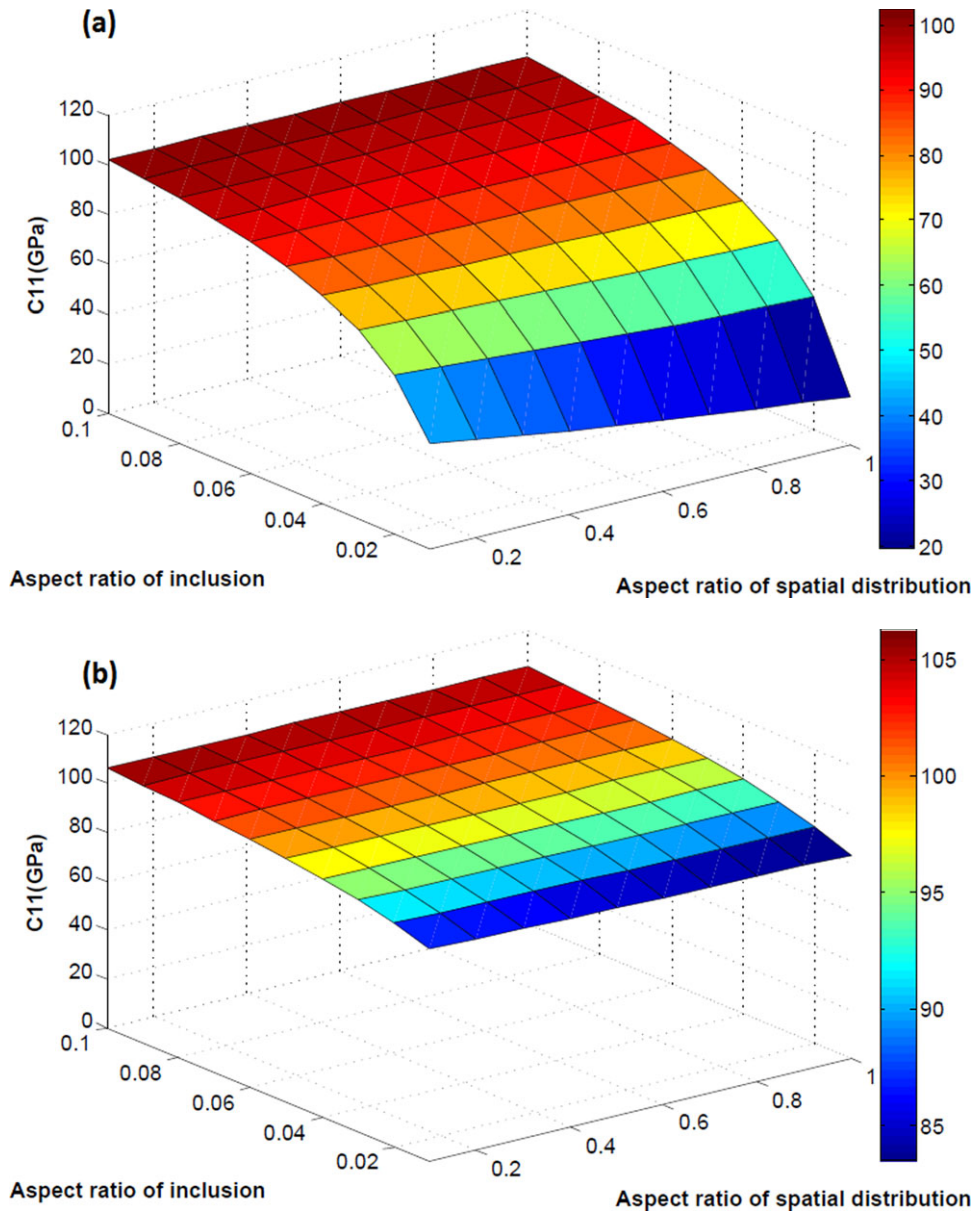


**Figure 8** Computed elastic stiffness  $C_{11}$  as a function of the aspect ratio of inclusion and the aspect ratio of spatial distribution. Porosity is set as 0.01. Data are colour-coded by the value of effective elastic stiffness. Cracks are assumed (a) dry and (b) brine saturated.

In Fig. 10, we use a numerical example to demonstrate that the effective elastic stiffness predicted by the compliance-based NIA is unphysical. We assume the aspect ratio of the inclusion is 1.0, suggesting that no anisotropy occurs in this case. When the porosity is 100%, theoretically, the effective bulk modulus of the rock should be zero, as the Kuster-Toksöz model and T-matrix predict. However, the compliance-based NIA increasingly overestimates the moduli as the porosity increases and this overestimation is evident from the fact that it

predicts finite elastic moduli when the porosity reaches 100%. Such an overestimate of effective elastic stiffness based on NIA was also reported by Hu and McMechan (2009) and Jaeger, Cook and Zimmerman (2007). In addition, this further demonstrates that there is an insufficient physical foundation to assume that the elastic interactions can be ignored at large concentrations of pores.

As displayed in Fig. 11, we also examine how the spatial distribution of cracks affects the seismic anisotropic

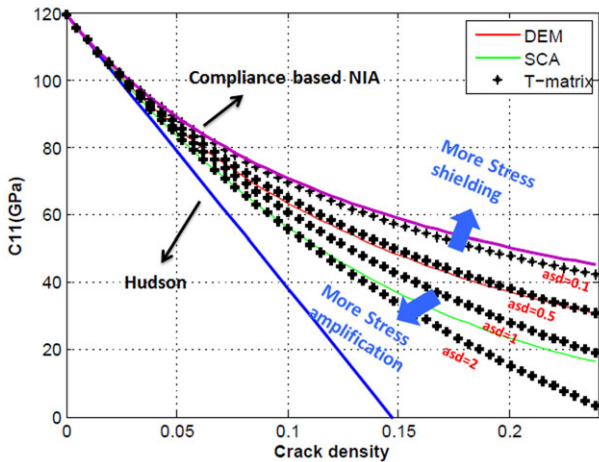


Figure 9 Comparison of C11 as a function of crack density predicted by different effective medium theories. The aspect ratio of the crack is set as 0.05. The blue, purple, red and green lines represent prediction by stiffness-based NIA, compliance-based NIA, DEM prediction and SCA prediction, respectively. The black dashed lines indicate the T-matrix prediction with different aspect ratios of spatial distribution.

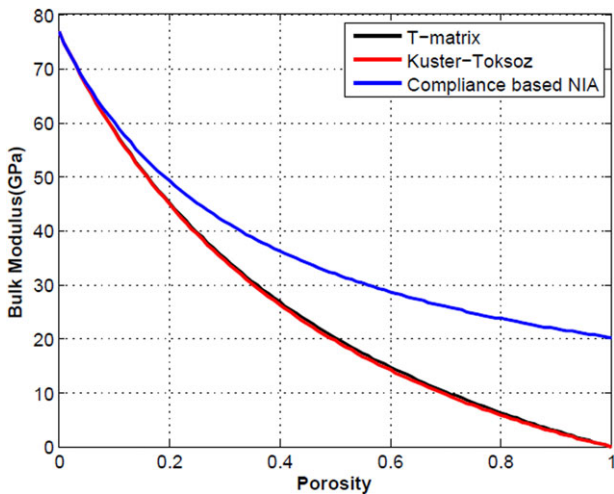


Figure 10 Elastic modulus of rocks containing dry, randomly distributed spherical pores, according to various effective medium theories. The red, black and blue lines represent predicted bulk modulus by the K-T model, T-matrix and compliance-based NIA, respectively. For T-matrix modelling, the aspect ratio of spatial distribution is set as 1.0.

parameters introduced for HTI media by Rüger (1997) and Tsvankin (1997). It is clear that the impacts of spatial distribution on seismic anisotropy become increasingly important when the inclusion concentrations increase beyond the dilute limit. Generally, the seismic anisotropy will increase as the aspect ratio of spatial distribution increases. In other words,

the stress amplification effect will enhance the amplitude of seismic anisotropy. In the real geological world, this may correspond to the fracture configuration where the cracks have a higher probability to appear in the vertical direction than the horizontal direction. Moreover, the gamma parameter, which is a measure of shear wave splitting that has been pointed out in many papers (e.g., Bakulin, Grechka and Tsvankin 2000), is approximate to crack density, which indicates the degree of fracturing. Figure 11(b) suggests that this approximation is reasonable only when the crack density is lower than 0.1. Nevertheless, at high crack density, when stress shielding dominates the crack interactions (the aspect ratio of the spatial distribution is small), the anisotropic parameter gamma gives a significantly higher estimate of crack density ( $|\gamma| < e$ ). From Fig. 11, we also observe that the elliptical anisotropy  $\eta = |\varepsilon - \delta|$ , which is an important parameter for P-wave time processing in anisotropic media, approximates to zero based on the compliance-based NIA. However, the T-matrix for a large aspect ratio of spatial distribution typically predicts positive elliptical anisotropy.

## DISCUSSION

The primary differences for the various inclusion and crack models presented here lie in their strategies for extrapolating the exact expression for deformation of a single ellipsoidal inclusion (Eshelby 1957) to handle the elastic interactions between inclusions (Mavko and Vanorio 2008). Theoretically, a good effective medium theory should satisfy two conditions. First of all, it should work beyond the dilute limit; secondly, it should characterize the pore and crack interactions with physical foundations. However, from the perspective of practical application, different effective medium theories can be selected according to the geological conditions. For example, DEM and SCA can work reasonably well for randomly distributed pores and cracks. For not heavily cracked reservoir rocks, the Hudson theory and compliance-based NIA can still be used to link crack density to the effective elastic properties with physical meaning. When dealing with pores or cracks having a certain distribution configuration, the T-matrix approach can offer a better prediction, which leads to higher accuracy for the effective elastic responses and seismic anisotropies. Nonetheless, given a real rock microstructure, it is often difficult to quantify the parameter concerning the spatial distribution of cracks or pores. Besides, it is obvious that the different spatial arrangements of cracks and the localization processes can make an impact on the crack

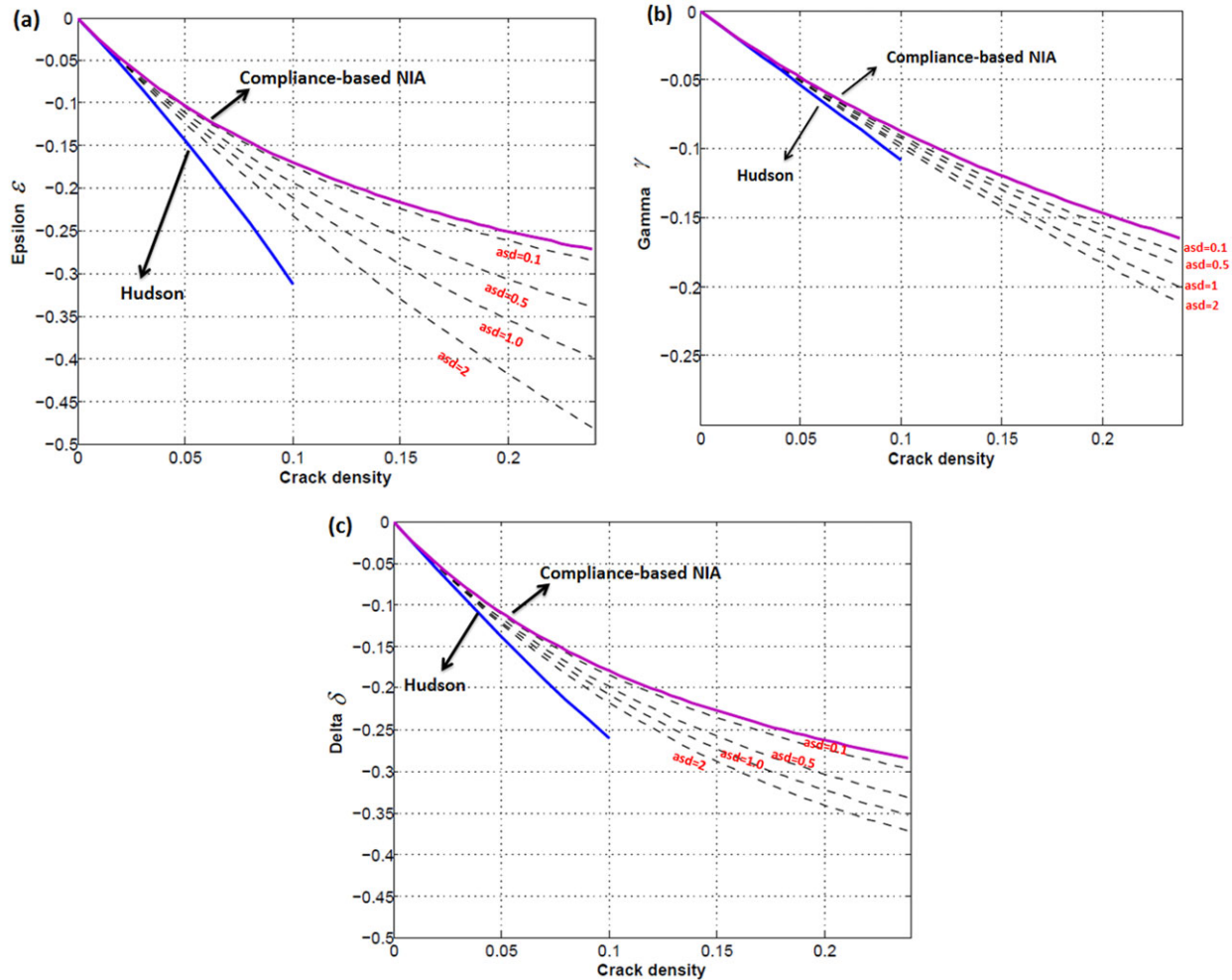


**Figure 11** Comparisons of predictions of Thomsen's anisotropic parameters as a function of crack density: (a) epsilon, (b) gamma and (c) delta. The blue and purple lines represent predictions by stiffness-based NIA and compliance-based NIA, respectively. The black dashed lines indicate T-matrix prediction with different aspect ratios of spatial distribution.

propagation and therefore the failure of the rock, which should be considered in future work.

The current approaches to understand and handle elastic interactions are based on the assumption that the pore and crack geometries are ellipsoidal. However, in real sedimentary rocks, pore and crack geometries are almost never ellipsoidal and often exhibit hopelessly complex and irregular microstructures. It is important to note that the stress interactions significantly depend on the details of the crack shape. For example, for smoothly tapered crack tips, the stress concentration and dilution can exhibit a quite different distribution compared with the case of ellipsoidal cracks and the resulting stress interactions and effective stiffness might also be significantly changed. Some attempts have been made to model effective elastic moduli when the pore shapes are not ellipsoidal

(Mavko and Nur 1978; Schoenberg 1980; Zimmerman 1991; Hudson and Liu 1999). As a consequence, the corresponding elastic interactions due to the different geometric features of cracks and pores should also be investigated in the future.

## CONCLUSIONS

The spatial arrangements of pores and cracks, which are mainly controlled and organized by geological processes, can naturally cause local elastic field variation and hence affect the effective elastic responses. We use the finite element modelling method to illustrate that stress amplification due to coplanar cracks significantly decreases the effective stiffness and the stress shielding due to stacked cracks significantly increases the effective stiffness. Rather than only using the volume

concentration and geometric features of pores and cracks, we suggest that the spatial arrangement of pores and cracks should be taken into account to compute the effective elastic properties. It is also demonstrated that the T-matrix approach, which explicitly takes into account the elastic interactions, can be used to better understand the elastic characteristics and seismic anisotropies due to varying spatial distributions of pores and cracks.

## ACKNOWLEDGEMENTS

This work was sponsored by the Fluids and DHI consortium of the Colorado School of Mines and the University of Houston and China National 973 Key Basic Research and Development Program (2014CB239006). The authors greatly appreciate Yves Guéguen and other anonymous reviewers for their constructive comments that significantly improved the work. Special thanks also go to Dr. Leon Thomsen and Dr. Enru Liu for their illuminating discussions.

## REFERENCES

- Bakulin A., Grechka V. and Tsvankin I. 2000. Estimation of fracture parameters from reflection seismic data – Part I: HTI model due to a single fracture set. *Geophysics* **65**, 1788–1802.
- Berryman J.G. 1980a. Long-wavelength propagation in composite elastic media. I Spherical inclusions. *Journal of the Acoustical Society of America* **68**, 1809–1819.
- Berryman J.G. 1980b. Long-wavelength propagation in composite elastic media. II Ellipsoidal inclusions. *Journal of the Acoustical Society of America* **68**, 1820–1831.
- Berryman J.G. 1992. Single-scattering approximations for coefficients in Biot's equations of poroelasticity. *Journal of the Acoustical Society of America* **91**, 551–571.
- Berryman J.G. 1995. Mixture theories for rock properties. In: *Rock Physics and Phase Relations: A Handbook of Physical Constants*, (ed. T.J. Ahrens), pp. 205–228. American Geophysical Union, Washington, D.C.
- Budiansky B. 1965. On the elastic moduli of some heterogeneous materials. *Journal of the Mechanics and Physics of Solids* **13**, 223–227.
- Eshelby J.D. 1957. The determination of the elastic field of an ellipsoidal inclusion and related problems. *Proceedings of the Royal Society of London, Series, A, Mathematical and Physical Sciences* **241**, 376–396.
- Grechka V. and Kachanov M. 2006. Effective elasticity of cracked rocks: A snapshot of the work in progress. *Geophysics* **71**(6), W45–W58.
- Guéguen Y. and Kachanov M. 2011. Effective elastic properties of cracked and porous rocks – An overview. *Mechanics of Crustal Rocks, CISM Courses and Lectures* **533**, 73–125.
- Hill L.R. 1965. A self-consistent mechanics of composite materials. *Journal of the Mechanics and Physics of Solids* **13**, 213–222.
- Hornby B.E., Schwartz L.M. and Hudson J.A. 1994. Anisotropic effective-medium modeling of the elastic properties of shales. *Geophysics* **59**, 1570–1583.
- Hu Y. and McMechan G.A. 2009. Comparison of effective stiffness and compliance for characterizing cracked rocks. *Geophysics* **74**(2), D49–D55.
- Hudson J.A. 1980. Overall properties of a cracked solid. *Mathematical Proceedings of the Cambridge Philosophical Society* **88**, 371–384.
- Hudson J.A. 1981. Wave speeds and attenuation of elastic waves in material containing cracks. *Geophysical Journal of the Royal Astronomical Society* **64**, 133–150.
- Hudson J.A. 1994. Overall properties of a material with inclusions or cavities. *Geophysical Journal International* **117**, 555–561.
- Hudson J.A. and Liu E. 1999. Effective elastic properties of heavily faulted structures. *Geophysics* **64**, 479–485.
- Jaeger J., Cook N.G. and Zimmerman R. 2007. *Fundamentals of Rock Mechanics*, 4th edn. Malden, MA, Blackwell Ltd.
- Jakobsen M. 2004. The interacting inclusion model of wave-induced fluid flow. *Geophysical Journal International* **158**, 1168–1176.
- Jakobsen M. and Chapman M. 2009. Unified theory of global flow and squirt flow in cracked porous media. *Geophysics* **74**(2), WA65–WA76.
- Jakobsen M., Hudson J.A. and Johansen T.A. 2003. T-Matrix approach to shale acoustics. *Geophysical Journal International* **154**, 533–558.
- Kachanov M. 1992. Effective elastic properties of cracked solids: Critical review of some basic concepts. *Applied Mechanics Reviews* **45**, 304–335.
- Kachanov M., Shafiro B. and Tsukrov I. 2003. *Handbook of Elasticity Solutions*. Kluwer Academic Publishers.
- Kachanov M., Tsukrov I. and Shafiro B. 1994. Effective moduli of solids with cavities of various shapes. *Applied Mechanics Reviews* **47**(1), S151–S174.
- Kuster G.T. and Toksöz M.N. 1974. Velocity and attenuation of seismic waves in two-phase media: Part I. Theoretical formulations. *Geophysics* **39**, 587–606.
- Liu E., Hudson J.A. and Pointer T. 2000. Equivalent medium representation of fractured rock. *Journal of Geophysical Research* **105**, 2981–3000.
- Mavko G. and Nur A. 1978. The effect of nonelliptical cracks on the compressibility of rocks. *Journal of Geophysical Research* **83**, 4459–4468.
- Mavko G., Mukerji T. and Dvorkin J. 2009. *The Rock Physics Handbook, Tools for Seismic Analysis in Porous Media*. Cambridge University Press
- Mavko G. and Vanorio T. 2008. Observation and limitations of effective medium models for pore shape. *Stanford Rock Physics & Borehole Geophysics Project Annual report* **114**(B9), 1–14
- Mura T. 1987. *Micromechanics of Defects in Solid*. Martinus Nijhoff Publishers.
- Nishizawa O. 1982. Seismic velocity anisotropy in a medium containing oriented cracks – Transversely isotropic case. *Journal of Physics of the Earth* **30**, 331–347.

- Norris A.N. 1985. A differential scheme for the effective moduli of composites. *Mechanics of Materials* 4, 1–16.
- O’Connell R.J. and Budiansky B. 1974. Seismic velocities in dry and saturated cracked solids. *Journal of Geophysical Research* 79, 5412–5426.
- Ponte Castañeda P. and Willis J.R. 1995. The effect of spatial distribution on the effective behavior of composite materials and cracked media. *Journal of Mechanics and Physics of Solids* 43, 1919–1951.
- Rüger A. 1997. P-wave reflection coefficients for transversely isotropic models with vertical and horizontal axis of symmetry. *Geophysics* 62, 713–722.
- Sayers C.M. and Kachanov M. 1995. Microcrack-induced elastic wave anisotropy of brittle rocks. *Journal of Geophysical Research* 100, 4149–4156.
- Schoenberg M. 1980. Elastic wave behavior across linear slip interfaces. *Journal of the Acoustic Society of America* 68, 1516–1521.
- Schoenberg M. 1983. Reflection of elastic waves from periodically stratified media with interfacial slip. *Geophysical Prospecting* 31, 265–292.
- Schoenberg M. and Douma J. 1988. Elastic wave propagation in media with parallel fractures and aligned cracks. *Geophysical Prospecting* 36, 571–590.
- Schoenberg M. and Sayers C.M. 1995. Seismic anisotropy of fractured rock. *Geophysics* 60, 204–211.
- Tsvankin I. 1997. Reflection moveout and parameter estimation for horizontal transverse isotropy. *Geophysics* 62, 614–629.
- Vernik L. and Kachanov M. 2010. Modeling elastic properties of siliciclastic rocks. *Geophysics* 75(6), E171–E182.
- Walsh J. 1965. The effects of cracks on the compressibility of rocks. *Journal of Geophysical Research* 70, 381–389.
- Wu T.T. 1966. The effect of inclusion shape on the elastic moduli of a two-phase material. *International Journal of Solids and Structures* 2, 1–8.
- Xu S. 1998. Modelling the effect of fluid communication on velocities in anisotropic porous rocks. *International Journal of Solids and Structures* 35, 4685–4707.
- Zimmerman R.W. 1991. Elastic moduli of a solid containing spherical inclusions. *Mechanics of Materials* 12, 17–24.